Notes

$M_3Ni_3Sb_4$ (M = Zr, Hf) and $Zr_3Pt_3Sb_4$. Ternary Antimonides with the $Y_3Au_3Sb_4$ Structure

Meitian Wang, Robert McDonald,† and Arthur Mar*

Department of Chemistry, University of Alberta, Edmonton, Alberta, Canada T6G 2G2

Received February 3, 1999

Introduction

Although $Y_3Au_3Sb_4$ was identified more than two decades ago,[1] its claim to fame lies in serving as the structure type adopted by many ternary pnictides $M_3M'_3Pn_4$ (Pn = As, Sb, Bi) and a few stannides $M_3M'_3Sn_4$ which have been the object of recent intense scrutiny because of their interesting electronic properties. The known compounds in this family generally consist of M = f-element and M′ = late transition metal (groups 9−11): $U_3M'_3Sb_4$ (M′ = Co, Rh, Ir),[2,3] $U_3Ni_{3-x}As_4$,[4] $M_3Ni_3Sb_4$ (M = U, Th),[2,3,5] $M_3Ni_3Sn_4$ (M = U, Th),[5−7] $U_3Pd_3Sb_4$,[2,5] $M_3Pt_3Sb_4$ (M = Ce−Nd, U),[2,5,8−10] $M_3Pt_3Bi_4$ (M = La, Ce),[11−13] $U_3Pt_3Sn_4$,[5] $M_3Cu_3Sb_4$ (M = Y, La−Nd, Sm, Gd−Er, U),[5,14−17] $U_3Cu_3Sn_4$,[5] $M_3Au_3Sb_4$ (M = Y, La−Nd, Sm, Gd−Lu),[1,8,9,18] and $U_3Au_3Sn_4$.[5] Some of these have been found to be Kondo insulators,[8−13] superconductors,[7] magnetoresistive materials,[13] and thermoelectric materials,[10,16] the properties originating from the f-electrons of the M component. Since doping is a common strategy for modifying electronic properties, the occurrence of isostructural compounds expands the range in which this is possible. We report here the preparation of $Zr_3Ni_3Sb_4$, $Hf_3Ni_3Sb_4$, and $Zr_3Pt_3Sb_4$, which represent the first members of this structural family that do *not* contain an f-element or Y for the M component.

Table 1. Cell Parameters for $M_3M'_3Sb_4$ (M = Zr, Hf; M′ = Ni, Pt)

compd	*a* (Å)	*V* (Å^3)
$Zr_3Ni_3Sb_4$	9.066(2)	745.1(4)
$Hf_3Ni_3Sb_4$	9.016(1)	732.8(4)
$Zr_3Pt_3Sb_4$	9.359(1)	819.8(4)

Table 2. Crystallographic Data for $Zr_3Ni_3Sb_4$

$Zr_3Ni_3Sb_4$	T_d^6-$I\bar{4}3d$ (No. 220)
fw 936.79	λ = 0.710 73 Å
a = 9.0617(6) Å[a]	ρ_{calcd} = 8.362 g cm^{-3}
V = 744.10(9) Å^3 [a]	μ(Mo Kα) = 255.9 cm^{-1}
Z = 4	$R(F)$ for $F_o^2 > 2\sigma(F_o^2)$[b] = 0.027
T = 22 °C	$R_w(F_o^2)$[c] = 0.065

[a] Based on 24 centered reflections in the range 16° ≤ 2θ(Mo Kα) ≤ 32° and obtained from a refinement constrained so that $a = b = c$ and $\alpha = \beta = \gamma = 90°$. [a] $R(F) = \sum||F_o| - |F_c||/\sum|F_o|$. [b] $R_w(F_o^2) = [\sum[w(F_o^2 - F_c^2)^2/\sum wF_o^4]^{1/2}$; $w^{-1} = [\sigma^2(F_o^2) + 6.72p]$ where $p = [\max(F_o^2,0) + 2F_c^2]/3$.

Experimental Section

Synthesis. Reactions were carried out on a ∼0.25-g scale by arc-melting mixtures of the elemental powders (Zr, 99.7%; Hf, 99.8%; Ni, 99.9%; Pt, 99.9%; all from Cerac) pressed into pellets. Each pellet was melted twice in a Centorr 5TA tri-arc furnace under argon (gettered by melting a titanium pellet) at slightly greater than atmospheric pressure. Single crystals of $Zr_3Ni_3Sb_4$ were originally found after arc-melting a mixture of Zr, Ni, and Sb in a 1:2:4.5 ratio and annealing in a Ta tube at 1000 °C for 5 days. EDX (energy-dispersive X-ray) analysis of these black block-shaped crystals on a Hitachi F2700 scanning electron microscope confirmed the presence of all three elements in roughly the expected proportions (23(2)% Zr, 34(2)% Ni, 43(2)% Sb). The X-ray powder patterns, obtained on an Enraf-Nonius FR552 Guinier camera (Cu Kα_1 radiation; Si standard), revealed the presence of $Zr_3Ni_3Sb_4$ as well as NiSb and Sb. A single crystal from this reaction was used for the structure determination described below.

Subsequently $Zr_3Ni_3Sb_4$, $Hf_3Ni_3Sb_4$, and $Zr_3Pt_3Sb_4$ could be prepared by arc-melting mixtures of the elements in stoichiometric proportions, with 2% excess Sb added to compensate for the weight loss suffered as a result of slight vaporization of Sb (2−4%). We were unable to prepare $Hf_3Pt_3Sb_4$, nor were we successful in substituting M = Nb, Ta or M′ = Co, Pd under these conditions. The cell parameters refined with the use of the program POLSQ[19] are listed in Table 1.

Structure Determination. Intensity data were collected at room temperature with the $\theta-2\theta$ scan technique in the range 11° ≤ 2θ(Mo Kα) ≤ 70° on an Enraf-Nonius CAD-4 diffractometer. Crystal data and further details of the data collection are given in Table 2 and the CIF. Calculations were carried out with the use of the SHELXTL (Version 5.1) package.[20] Conventional atomic scattering factors and anomalous dispersion corrections were used.[21] Intensity data were processed and face-indexed absorption corrections were applied in XPREP. The unique space group consistent with the cubic symmetry

† Faculty Service Officer, Structure Determination Laboratory.

(1) Dwight, A. E. *Acta Crystallogr., Sect. B: Struct. Crystallogr. Cryst. Chem.* **1977**, *33*, 1579.
(2) Dwight, A. E. *J. Nucl. Mater.* **1979**, *79*, 417.
(3) Buschow, K. H. J.; de Mooij, D. B.; Palstra, T. T. M.; Nieuwenhuys, G. J.; Mydosh, J. A. *Philips J. Res.* **1985**, *40*, 313.
(4) Troc, R.; Kaczorowski, D.; Noël, H.; Guerin, R. *J. Less-Common Met.* **1990**, *157*, L1.
(5) Takabatake, T.; Miyata, S.-I.; Fujii, H.; Aoki, Y.; Suzuki, T.; Fujita, T.; Sakurai, J.; Hiraoka, T. *J. Phys. Soc. Jpn.* **1990**, *59*, 4412.
(6) Yethiraj, M.; Robinson, R. A.; Rhyne, J. J.; Gotaas, J. A.; Buschow, K. H. J. *J. Magn. Magn. Mater.* **1989**, *79*, 355.
(7) Aoki, Y.; Suzuki, T.; Fujita, T.; Takabatake, T.; Miyata, S.-I.; Fujii, H. *J. Phys. Soc. Jpn.* **1992**, *61*, 684.
(8) Kasaya, M.; Katoh, K.; Takegahara, K. *Solid State Commun.* **1991**, *78*, 797.
(9) Kasaya, M.; Katoh, K.; Kohgi, M.; Osakabe, T.; Sato, N. *Physica B* **1994**, *199*−*200*, 534.
(10) Jones, C. D. W.; Regan, K. A.; DiSalvo, F. J. *Phys. Rev. B: Condens. Matter* **1998**, *58*, 16057.
(11) Hundley, M. F.; Canfield, P. C.; Thompson, J. D.; Fisk, Z.; Lawrence, J. M. *Phys. Rev. B: Condens. Matter* **1990**, *42*, 6842.
(12) Severing, A.; Thompson, J. D.; Canfield, P. C.; Fisk, Z.; Riseborough, P. *Phys. Rev. B: Condens. Matter* **1991**, *44*, 6832.
(13) Hundley, M. F.; Lacerda, A.; Canfield, P. C.; Thompson, J. D.; Fisk, Z. *Physica B* **1993**, *186*−*188*, 425.
(14) Skolozdra, R. V.; Salamakha, P. S.; Ganzyuk, A. L.; Bodak, O. I. *Izv. Akad. Nauk SSSR, Neorg. Mater.* **1993**, *29*, 25.
(15) Patil, S.; Hossain, Z.; Paulose, P. L.; Nagarajan, R.; Gupta, L. C.; Godart, C. *Solid State Commun.* **1996**, *99*, 419.
(16) Fess, K.; Kaefer, W.; Thurner, Ch.; Friemelt, K.; Kloc, Ch.; Bucher, E. *J. Appl. Phys.* **1998**, *83*, 2568.
(17) Fujii, H.; Miyata, S.; Takabatake, T. *J. Magn. Magn. Mater.* **1992**, *104*−*107*, 45.
(18) Katoh, K.; Kasaya, M. *Physica B* **1993**, *186*−*188*, 428.
(19) POLSQ: Program for least-squares unit cell refinement. Modified by D. Cahen and D. Keszler, Northwestern University, 1983.
(20) Sheldrick, G. M. *SHELXTL*, version 5.1; Bruker Analytical X-ray Instruments, Inc.: Madison, WI, 1997.
(21) *International Tables for X-ray Crystallography*; Wilson, A. J. C., Ed.; Kluwer: Dordrecht, The Netherlands, 1992; Vol. C.

10.1021/ic990144i CCC: $18.00
Published on Web 06/24/1999

Table 3. Positional and Equivalent Isotropic Thermal Parameters (Å^2) for $Zr_3Ni_3Sb_4$

atom	Wyckoff position	*x*	*y*	*z*	U_{eq}[a]
Zr	12a	$^3/_8$	0	$^1/_4$	0.0082(3)
Ni	12b	$^7/_8$	0	$^1/_4$	0.0075(4)
Sb	16c	0.08207(6)	0.08207(6)	0.08207(6)	0.0067(2)

[a] U_{eq} is defined as one-third of the trace of the orthogonalized $\boldsymbol{U}_{ij}$ tensor.

Table 4. Extended Hückel Parameters

atom	orbital	H_{ii} (eV)	ξ_{i1}	c_1	ξ_{i2}	c_2
Zr	5s	−8.52	1.82			
	5p	−4.92	1.78			
	4d	−8.63	3.84	0.6213	1.510	0.5798
Ni	4s	−8.03	1.93			
	4p	−3.74	1.93			
	3d	−9.90	5.75	0.5817	2.20	0.5800
Sb	5s	−18.80	2.32			
	5p	−11.70	2.00			

and the systematic absences in the intensity data is $I\bar{4}3d$. All atoms were easily found by direct methods, and the structure was refined by least-squares methods. All sites are fully occupied, as confirmed by refinements on the occupancies, which converge to 99(7)% for Zr, 100(7)% for Ni, and 100(7)% for Sb, with reasonable displacement parameters. The Flack parameter converges to −0.04(8), confirming the correct absolute structure. The final cycle of least-squares refinement on F_o^2 of 9 variables (including anisotropic displacement parameters and an isotropic extinction parameter) and 276 averaged reflections (including those having $F_o^2 < 0$) converged to values of $R_w(F_o^2)$ of 0.065 and $R(F)$ (for $F_o^2 > 2\sigma(F_o^2)$) of 0.027. The final difference electron density map is featureless ($\Delta\rho_{max} = 1.28$; $\Delta\rho_{min} = -1.19$ e Å^{-3}). Final values of the positional and equivalent isotropic displacement parameters are given in Table 3, anisotropic displacement parameters and full metrical details are in the CIF, and final structure amplitudes are available from A.M.

Band Structure. Extended Hückel calculations[22,23] were carried out using the EHMACC suite of programs to determine the band structure of $Zr_3Ni_3Sb_4$. The atomic parameters used were taken from those previously applied to ZrNiSb and are listed in Table 4.[24] Properties were extracted from the band structure using 40 *k*-points in the irreducible portion of the Brillouin zone.

Results and Discussion

The known ternary zirconium and hafnium nickel antimonides, MNiSb,[24] MNi_2Sb,[25,26] M_5NiSb_3 (M = Zr, Hf),[27,28] $Zr_5Ni_{0.7}Sb_{2.3}$,[29] and $Hf_6Ni_{1-x}Sb_{2+x}$,[30] are all metal-rich phases, and the compounds $M_3Ni_3Sb_4$ (M = Zr, Hf) which extend these ternary systems are no exception. To our knowledge, $Zr_3Pt_3Sb_4$ is the first ternary zirconium platinum antimonide. While the $M_3Ni_3Sb_4$ composition is close to being equiatomic, we did not observe the formation of the known MNiSb (M = Zr, Hf)[24] as a competing phase under the synthetic conditions used. In contrast, attempts to substitute Ni with Co resulted in the formation of MCoSb (M = Zr, Hf) with the LiAlSi-type structure.[24,31]

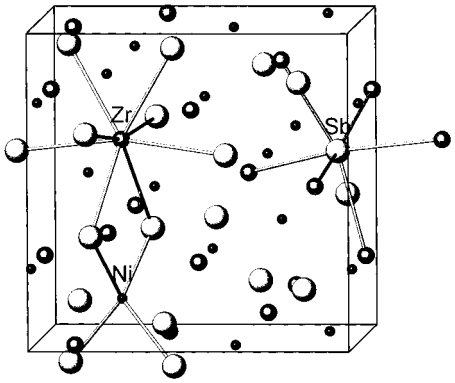

Figure 1. View of $Zr_3Ni_3Sb_4$ with the cubic unit cell outlined. The medium spheres are Zr atoms, the small dark spheres are Ni atoms, and the large light spheres are Sb atoms. A Zr-centered dodecahedron, a Ni-centered tetrahedron, and an Sb-centered octahedron are highlighted.

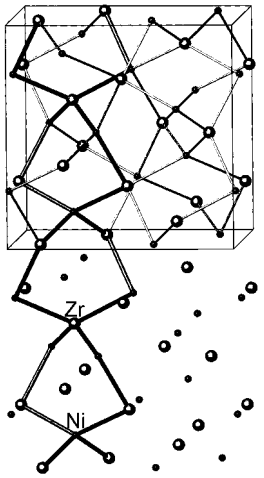

Figure 2. View of the Zr−Ni bonding network in $Zr_3Ni_3Sb_4$, with all Sb atoms omitted for clarity. The medium lighter spheres are Zr atoms, and the small dark spheres are Ni atoms. One of the chains of six-membered rings running parallel to a $\bar{4}$ axis is outlined with thicker bonds, extending into the next unit cell.

$Zr_3Ni_3Sb_4$ adopts the $Y_3Au_3Sb_4$ structure, a filled variant of the more prevalent Th_3P_4 structure. These are complicated structures which defy a straightforward description.[32,33] As shown in Figure 1, the Zr atom is coordinated to eight Sb atoms at 3.1240(6)−3.1488(6) Å in a dodecahedron (or more accurately, a bisdisphenoid (two interpenetrating tetrahedra) because the two sets of Zr−Sb distances are inequivalent), while the Ni atom is coordinated to four Sb atoms at 2.5278(3) Å in a tetrahedron elongated along its $\bar{4}$ axis. The Zr−Sb and Ni−Sb distances are comparable to those found in ZrNiSb (2.9144(7)−3.3212(7) Å and 2.4858(6)−2.617(1) Å, respectively).[24] The "Zr_3Sb_4" part of $Zr_3Ni_3Sb_4$ corresponds to the Th_3P_4 structure, which consists of an array of metal-centered dodecahedra sharing edges and faces in all directions.[33] Filling all the remaining tetrahedral sites between the dodecahedra with Ni atoms results in the space-filling array of the $Y_3Au_3Sb_4$ structure adopted by $Zr_3Ni_3Sb_4$. Understandably, this traditional structural description of metal-centered polyhedra is difficult to represent clearly in a figure. An alternative description considers the anionic substructure, which consists of two

(22) Hoffmann, R. *J. Chem. Phys.* **1963**, *39*, 1397.
(23) Whangbo, M.-H.; Hoffmann, R. *J. Am. Chem. Soc.* **1978**, *100*, 6093.
(24) Kleinke, H. *Z. Anorg. Allg. Chem.* **1998**, *624*, 1272.
(25) Soltys, J.; Turek, K. *Acta Phys. Pol. A* **1975**, *47*, 335.
(26) Dwight, A. E. *Mater. Res. Bull.* **1987**, *22*, 201.
(27) Rieger, W.; Parthé, E. *Acta Crystallogr., Sect. B: Struct. Crystallogr. Cryst. Chem.* **1968**, *24*, 456.
(28) Garcia, E.; Corbett, J. D. *Inorg. Chem.* **1990**, *29*, 3274.
(29) Kwon, Y.-U.; Sevov, S. C.; Corbett, J. D. *Chem. Mater.* **1990**, *2*, 550.
(30) Kleinke, H. *J. Alloys Compd.* **1998**, *270*, 136.
(31) Marazza, R.; Ferro, R.; Rambaldi, G. *J. Less-Common Met.* **1975**, *39*, 341.
(32) Pearson, W. B. *The Crystal Chemistry and Physics of Metals and Alloys*; Wiley: New York, 1972.
(33) Hyde, B. G.; Andersson, S. *Inorganic Crystal Structures*; Wiley: New York, 1989.

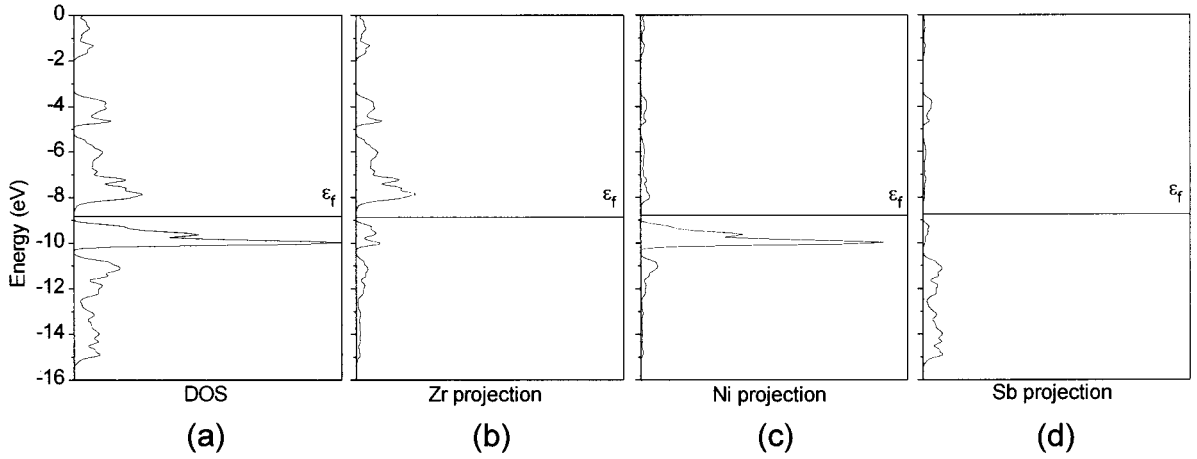

Figure 3. (a) Total density of states (DOS) curve for $Zr_3Ni_3Sb_4$ and its (b) Zr, (c) Ni, and (d) Sb projections.

interpenetrating enantiomeric three-connected nets of the nonmetal component.[34] In the present case, because the Sb−Sb distances are all greater than 3.3 Å and are shown to be nonbonding (see below), such a description does not accurately portray the bonding network within the $Zr_3Ni_3Sb_4$ structure. On the other hand, given the short Zr−Ni distances of 2.7746(2) Å, metal−metal bonding is undoubtedly an integral part of this structure. (Being the most electronegative component, Sb is regarded as the nonmetal, in a Zintl-type approximation.) As shown in Figure 2, the Zr and Ni atoms are tetrahedrally surrounded by atoms of the other kind to form a four-connected net extending in all three directions, with the tetrahedra sharing edges. This net can be decomposed into chains, one of which is drawn in isolation in the bottom half of Figure 2. These chains run along $\bar{4}$ axes, parallel to each of the cubic axes, and form six-membered rings in a twist-boat conformation. The Sb atoms are then located at the centers of highly distorted octahedra (Figure 1) whose vertexes are the Zr atoms.

The synthesis of $Zr_3Ni_3Sb_4$ raises questions about the contribution of metal−metal bonding in $M_3M'_3Pn_4$ compounds. For M = lanthanide or Y, and more so for M = actinide, the M−M′ distance can be quite short, certainly within the realm of metal−metal bonding (e.g., d(Nd−Cu) = 2.96 Å in $Nd_3Cu_3Sb_4$,[14] d(Y−Au) = 3.006(1) Å in $Y_3Au_3Sb_4$,[1] and d(U−Ni) = 2.874(1) Å in $U_3Ni_3Sb_4$[2]). In contrast to the cases above in which the degree of metal−metal bonding or the contribution of f-orbitals vs d-orbitals to bonding can be debated, the Zr−Ni bonding in $Zr_3Ni_3Sb_4$ inarguably has a strong covalent character and necessarily results from overlap of d-orbitals. Given that Zr−Ni distances of 2.9131(7)−3.138(1) Å in ZrNiSb and 2.6951(8)−2.807(2) Å in $Zr_9Ni_2P_4$ correspond to not insignificant Mulliken overlap populations of 0.05−0.10 and 0.06−0.21, respectively,[24,35] the short distance of 2.7746(2) Å in $Zr_3Ni_3Sb_4$ implies a substantial bonding interaction. It is noteworthy that, (i) except for $U_3Pd_3Sb_4$,[2,5] no other $M_3M'_3Sb_4$ phases have been found with M′ = Pd and (ii) the compound "$Hf_3Pt_3Sb_4$" could not be prepared. This suggests that there may be some optimum degree of metal−metal bonding for the $Y_3Au_3Sb_4$ structure to exist. To test this proposal, we have carried out a band structure calculation on $Zr_3Ni_3Sb_4$.

The total density of states (DOS) curve (Figure 3a) shows that $Zr_3Ni_3Sb_4$ is predicted to be a semiconductor with a small band gap of 0.57 eV. Although infrared (4000−400 cm^{-1}) diffuse reflectance measurements on a powder sample of $Zr_3Ni_3Sb_4$ did not reveal any absorption that would suggest a band gap, it should be noted that the extended Hückel method is rarely accurate enough to yield correct band gap energies. The presence of impurities can well introduce donor or acceptor levels that mask the intrinsic band gap energy, which would be difficult to measure by optical methods. At best, we can conclude that $Zr_3Ni_3Sb_4$ is a narrow-gap semiconductor or a semimetal. Lack of suitably large single crystals has precluded electrical measurements thus far.

The electron count in $Zr_3Ni_3Sb_4$ ($3 \times 4 + 3 \times 0 + 4 \times 5$) preserves the value of 32 e^- per formula unit found in many $M_3M'_3Pn_4$ compounds.[14] By analogy with $Th_3Ni_3Sb_4$,[5] an approximation to an oxidation state formalism for $Zr_3Ni_3Sb_4$ would be "$(Zr^{+4})_3(Ni^0)_3(Sb^{-3})_4$." While Sb^{-3} appears to be consistent with the presence of isolated Sb atoms within the structure, clearly Zr^{+4} represents an unrealistic extreme, and a reduced actual charge would be expected for Zr−Ni bonding to occur. Figure 3b shows that Zr 4d states contribute largely to the unoccupied conduction band (above −8.5 eV), but there are important contributions to the filled states at lower energy as well. Most of the Ni 3d states contribute to the large narrow peak in the DOS (between −10.5 and −9 eV) (Figure 3c), which constitutes the valence band, implying a nearly d^{10} configuration for Ni. The bands between −15.5 and −10.5 eV have contributions from all three atom types, with Sb 5p character being dominant (Figure 3d), and these correspond to strong metal−nonmetal bonding states in $Zr_3Ni_3Sb_4$. The calculated charges are +0.53 for Zr, −0.07 for Ni, and −0.35 for Sb. Importantly, the reduced charge on Zr sets up a situation for metal−metal bonding to occur with Ni.

Crystal orbital overlap population (COOP) curves (Figure 4) were analyzed to quantify the degree of bonding in $Zr_3Ni_3Sb_4$. As expected, there are strong Zr−Sb and Ni−Sb bonds, corresponding to large Mulliken overlap populations (MOP) of 0.266 and 0.245, respectively. To provide a reference for Zr−Ni bond strengths, the band structure of the binary intermetallic ZrNi[36] was also determined.[37] The MOP of 0.156 for the Zr−Ni bond (2.7746(2) Å) in $Zr_3Ni_3Sb_4$ is significant, when compared to an MOP of ∼0.20 for the Zr−Ni bonds (2.74 Å) in ZrNi. Although Sb−Sb contacts as long as the 3.3875(6) Å distance found in $Zr_3Ni_3Sb_4$ have been implicated as weakly

(34) Heim, H.; Bärnighausen, H. *Acta Crystallogr., Sect. B: Struct. Crystallogr. Cryst. Chem.* **1978**, *34*, 2084.
(35) Kleinke, H.; Franzen, H. F. *Inorg. Chem.* **1996**, *35*, 5272.
(36) Kirkpatrick, M. E.; Bailey, D. M.; Smith, J. F. *Acta Crystallogr.* **1962**, *15*, 252.
(37) Wang, M.; Mar, A. Unpublished results.
(38) Kleinke, H. *Eur. J. Inorg. Chem.* **1998**, 1369.

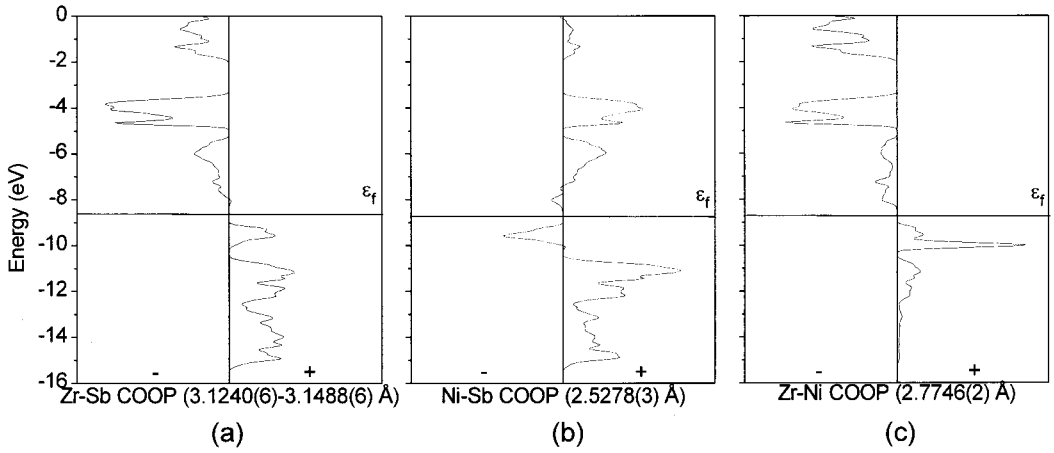

Figure 4. Crystal orbital overlap population (COOP) curves for (a) Zr−Sb, (b) Ni−Sb, and (c) Zr−Ni contacts in $Zr_3Ni_3Sb_4$.

bonding in other antimonides, such as $Zr_2V_6Sb_9$,[38] the MOP of 0.025 here implies negligible, if any, Sb−Sb bonding. $Zr_3Ni_3Sb_4$ provides a useful comparison to ZrNiSb,[24] being close in composition. The key difference seems to be that the modest Zr−Zr bonding (MOP 0.159) in ZrNiSb disappears on going to $Zr_3Ni_3Sb_4$. While Ni−Sb bond strengths are similar in both compounds, the weaker Zr−Sb bonds and the absence of Zr−Zr bonds (all Zr−Zr interatomic distances are greater than 4 Å) in $Zr_3Ni_3Sb_4$ are compensated by the presence of stronger Zr−Ni bonds.

In conclusion, we have demonstrated that metal−metal bonding (Zr−Ni) is an important feature in $Zr_3Ni_3Sb_4$, and we propose that it may be equally significant, by extension, to other $M_3M'_3Pn_4$ compounds, particularly those with M = U or Th. Since the unusual electronic properties of many $M_3M'_3Pn_4$ compounds are believed to originate from f-orbital participation when M is a lanthanide or actinide (particularly Ce and U, which have a stable +4 oxidation state), it will be interesting to see how these properties change when Zr, which only has d-electrons available, is partially substituted for these elements.

Acknowledgment. This work was supported by the Natural Sciences and Engineering Research Council of Canada and the University of Alberta.

Supporting Information Available: A listing of X-ray powder diffraction data. One X-ray crystallographic file, in CIF format. This material is available free of charge via the Internet at http://pubs.acs.org.

IC990144I